



THERMAL CHARACTERISTICS OF PHASE CHANGE MATERIAL USED AS THERMAL STORAGE SYSTEM BY USING SOLAR ENERGY

Kadhim F. Nasir¹, Munir Ali² and Ameer H. AL Mamoori³

¹ PhD, Farm Machinery and Equipment Eng. Dept., AL Mussaib Technical College, AL Furat Alawsat Technical University, Email: kka_ff70@yahoo.com,

² PhD, Ankara Yildirim Beyazit University, Email: monierelfarra@hotmail.com

³ Mechanical Dept., AL Mussaib Technical Institute, AL Furat Alawsat Technical University, Email: aemirhassan48@gmail.com

<http://dx.doi.org/10.30572/2018/kje/090101>

ABSTRACT

In this paper, the melting processes of phase change material in a shell and tube heat exchanger by using solar thermal energy have been investigated numerically and experimentally. All experimental were outdoor tested at AL-Mussaib city-Babylon-Iraq (Lat 32.5 ° North, and long 44.3 ° East) with N-S collector direction at tilt angle of 32.5 ° with the horizontal. The phase change material used in this work is black color Iraqi origin pure Paraffin with amount of 12 kg. In the experimental setup evacuated tube solar collector is employed for melting phase change material in shell regime. Different volume flow rates for the water flow inside the inner tube of heat exchanger namely (200, 300, and 500 LPH) for Reynolds number namely (15000, 23000, 38000) respectively were used for each season from August 2016 to January 2017. The numerical investigation involves a three dimension numerical solution of model by a commercial package ANSYS FLUENT 15.0. The boundary conditions of the model that solved by the numerical solution have been taken from the experimental tests. The experimental results indicated that the inner tube inlet and ambient temperatures has a significant effects on the melting process compared with the volume flow rates. Studying phase change material temperature distribution, it is exposed that a melting temperature of the phase change material in summer season needed time of (3-4) hours only, while it needed more time; (14-16) hours in winter season. Increasing solar radiation and ambient temperature reduces the melting time of phase change material. Increasing water temperature difference of inner tube increased the heat gained for phase change material. The results obtained from numerical solution presented the static temperature contours and showed that the temperature distribution of phase change material give good validations with experimental results with percentage deviation of 2.7%. The present experimental results have been compared with the previous studies and give a good agreement with increasing for present work of 25.9 %.

KEY WORDS: phase change material, paraffin, solar energy, shell and tube, heat exchanger

الخواص الحرارية للمواد متغيرة الاطوار المستخدمة كنظام خزن حراري باستعمال الطاقة الشمسية

د. كاظم فاضل ناصر¹، د. منير علي²، امير حسن حمزة المعموري³

¹ قسم هندسة تقنيات المكنائ والمعدات الزراعية / جامعة الفرات الاوسط التقنية / الكلية التقنية – المسيب، ² جامعة انقرة بايزيد يلدريم، ³ جامعة مؤسسة تركيا للطيران.

الخلاصة

في هذه البحث تم دراسة عملية وعددية لعمليات انصهار المواد متغيرة الاطوار باستخدام الطاقة الشمسية في مبادل حراري من نوع الغلاف والانبوب. انجزت الدراسة العملية في الاجواء الخارجية بمدينة المسيب- محافظة بابل- العراق (خط عرض 32.5° شمالاً وخط طول 44.3° شرقاً) عند زاوية ميلان 32.5° مع الافق باتجاه الجنوب خلال الفترة من شهر اب 2016 الى كانون الثاني 2017. تضمن الجانب العملي استخدام مجمع شمسي من نوع الانابيب المتفرغة بدون استخدام منظومة توجيه لصفحة المادة متعددة الاطوار. استخدم البرافين النقي اسود اللون وعراقي الانتاج بكمية 12 كيلو غرام كمادة متغيرة الاطوار في منطقة الغلاف. استخدمت معدلات تدفق متغيرة للماء داخل الانبوب للمبادل الحراري وهي 200, 300, و500 لتر لكل ساعة. الدراسة النظرية تضمنت عمل محاكات باستخدام برنامج ANSYS FLUENT 15.0 لنموذج يمثل المبادل الحراري، الظروف الحدية للنموذج اخذت من التجارب العملية. اظهرت النتائج المستحصلة من الاختبارات العملية ان درجة حرارة الماء الداخل للانبوب الداخلي للمبادل الحراري ودرجة حرارة الطقس لها تأثير كبير في عملية انصهار المادة متغيرة الاطوار مقارنة بتأثير معدلات جريان الماء. واطهرت النتائج ان عملية انصهار البرافين في فصل الصيف تحتاج الى فترة زمنية مقدارها 3-4 ساعة فقط بينما تحتاج في فصل الشتاء الى فترة زمنية مقدارها 14-16 ساعة، زيادة الاشعاع الشمسي ودرجة حرارة الطقس تؤدي الى تقليل الفترة الزمنية اللازمة لانصهار البرافين. اظهرت النتائج النظرية تطابقاً مع النتائج العملية لدرجات حرارة البرافين مع فرق مقداره 2,7%. تم مقارنة النتائج العملية لهذه الدراسة مع نتائج بحوث سابقة في مجال انصهار المواد متغيرة الاطوار وقد اظهرت المقارنة افضلية جيدة في النتائج للدراسة الحالية بنسبة 25,9% زيادة في درجات حرارة البرافين.

NOMENCLATURE

| Symbol | Definition | Units | Greek symbols | Definition | Units |
|----------------|-------------------------------------|------------------|---------------|-------------------------|-------------------|
| A | Area, apparent | m ² | ρ | density | Kg/m ³ |
| C _p | Specific heat | J/kg.k | η | Efficiency of collector | - |
| d | Diameter of the tube | m | Subscripts | - | - |
| I | Incident solar radiation, | W/m ² | <i>a</i> | Air, ambient, aperture | - |
| Q | Heat transfer rate | m | <i>i</i> | Collector Inlet | - |
| QL | Latent Heat | W | <i>in</i> | Inner tube Inlet | - |
| Q _u | Useful energy gained from collector | W | <i>o</i> | Collector Outlet | - |
| T | Temperature | °C | <i>out</i> | Inner tube outlet | - |
| V | velocity | m/s | | | |
| \dot{m} | Mass flow rate | Kg/s | | | |

1. INTRODUCTION

Thermal energy storage (TES) is presented as the temporary holding of thermal energy in the form of cold or hot substances for later use. Energy request change on seasonal, weekly and daily, bases. These request can be matched with the help systems that a labor synergistically,, and the agree with the storage of energy by heating, cooling ,melting, vaporizing or solidifying a material and the thermal energy be obtainable when the process is reversed. A considerable technology in systems included renewable energies as well as other energy resources as it can make their a process more efficient, particularly by bridging the interval between intervals when energy is harvested and intervals when it is necessary. That is beneficial for balancing between the equipping and request of energy (Fernandez, 2012). Thermal Energy Storage is foundation to overcome the mismatches between the equipping and consumption of energy or primary energy o source divergence. Such as patrol variations of solar energy. Phase Change Material (PCM) used for Latent Heat Storage has received senior attention attributed to its isothermal nature and density high storage and of heat storage and release. There are many type of PCM. Applications such as; heat utilization, and water heating, waste and space air conditioning, and cooling and thermal oversight applications (Ravikumar and Pss., 2008). The numerous PCMs are categorized as organic, inorganic and eutectic materials, which can be identified as PCM from the point of view of melting temperature and latent heat of fusion. Of these, PCMs with a melting point between 20–60 °C are applicable to residential building using radiant floor heating systems (Abhat, 1983).

Shuo et al., (2004) was investigated low melt temperature paraffin as a phase change material (PCM) and describing of a group of thermal energy storage (TES) composites that combine TES and structural functionality was showed. A thermoplastic SEBS/paraffin and three different epoxy systems system with different glass transition temperatures were studied. Epoxy matrices were used to encapsulate Paraffin particles. The thermal conductivity, particle size distribution, thermal diffusivity, contact resistance, and latent heat of the composites were measured. It was noted that the thermal conductivity of the composites was increased when the phase change material was a liquid, partly because of best wetting of the epoxy by the liquid paraffin and because volume expansion of the paraffin liquid in the composite. The interaction between components of paraffin/epoxy, provide appropriate thermal and mechanical performance. The thermoplastic SEBS/paraffin system display excellent mechanical performance and thermal (Kenisarin and Mahkamov, 2007), were focused on various PCMs thermal properties and its assessment on heat storage design configurations facilities and

methods of heat transfer enhancement that were used as a part of solar active and passive space heating systems, solar cooking and greenhouses. The analysis of data published in the open previous literature led to the following conclusions. Differential thermal analysis and differential scanning calorimetry methods were the main methods used in studying the thermal properties of PCM and considerably differ from strict thermo-physical methods (Sharma and Chen, 2009), summarized the investigation of the solar water heating system incorporating with Phase Change Materials Suitable PCM became specified easily and provided several designs for solar water heating systems. (Bhatt et al., 2010), reviewed more than sixty phase changing materials including inorganic, organic, eutectic and ionic liquids with considering to the capacity of their thermal energy storage. The study based on properties like heat of fusion, melting temperature, density and thermal conductivity. These prepared a list of nine favorable phase changing materials, suitable for thermal energy storage (Warzoha et al., 2012), investigated experimentally the effect of infiltration method on paraffin PCM saturation rate within graphite foams. The foam was infiltrated by two methods: a vacuum infiltration technique and a simple submersion technique. Paraffin when infiltrated graphite foams, became effective for energy storage, but the foam was not easy saturated with paraffin. The influence of the infiltration method on the rate of paraffin saturation was found, yielding better results with the vacuum system (Sinaringati et al., 2016), investigated experimentally the utilization of the paraffin and beeswax materials as a heat energy sources for infant incubator and made comparison between them. The results showed that the phase change material can keep heat energy in the infant incubator room at temperature above 32°C for more than 8 hours. The beeswax performed better heat energy storage than paraffin and best performance when used beeswax as the PCM for infant incubator or any other practical application.

The aim of this work is investigation the effect of using solar energy on the thermal characteristics of Phase change materials (PCM) which used for providing storage thermal energy under outdoor test for Iraq climate conditions at AL-Mussaib city-Babylon-Iraq (Lat 32.5 ° North, and long 44.3 ° East).

2. EXPERIMENTAL SETUP

2.1. Experimental rig

The Experimental rig includes vacuum tubes solar collector (VTSC) using with shell and tube heat exchanger is designed and fabricated in order to study the effect of different ambient conditions and collector water flow conditions on the thermal performance of PCM. The experimental rig and a schematic diagram of the comprehensive experimental system are shown

in Figs. 1 and 2, respectively. The experimental rig specifications consists of: solar Water collector; This collector is evacuated tube type consists of storage tank of 80 liter capacity and 12 evacuated tube as shown in the Fig. 1, shell and tube heat exchanger; which consists of rectangular tube and circular cylinder as shell, electrical AC water pumps to circulate water, connecting plastic pipes of (3/4 inch) to connect the parts of the setup system, glass wool insulations has a thickness of 15 mm to insulate all system pipes, and global valves for controlling the amount of water flow and Senior safety valves system used for preventing exposed to high-pressure upon the arrival of water at high temperatures.



Fig. 1. The experimental rig.

2.2. Measurements and Instrumentation

The measurement devices that used in this work includes: Ten standard thermocouples type (K) with 0.4 mm diameter and 1 m long its locations distributed in the test rig are shown in Fig. 2 are used in this work which connected to Digital data logger type of 12 channels temperature recorder with an accuracy of ($\pm 4\%$). Nuritech flowmeter with range of (1.8-19 lpm) to measure water volumetric flow rate, Kipp and Zonen Pyranometer having a measuring range of up to 4000 W/m^2 to measure solar intensity which installed on the collector at tilt angle of 32.5° with the horizontal, and Lutron multifunctional anemometer device to measure the wind speed and with measurement range of (0.4-30) m/s.

2.3. Phase Change Materials

There is one type of PCM used in this work, the type is black Iraqi origin pure Paraffin with amount of 12 kg which shown in the Fig. 3. The physical properties of PCM are shown in Table 1.

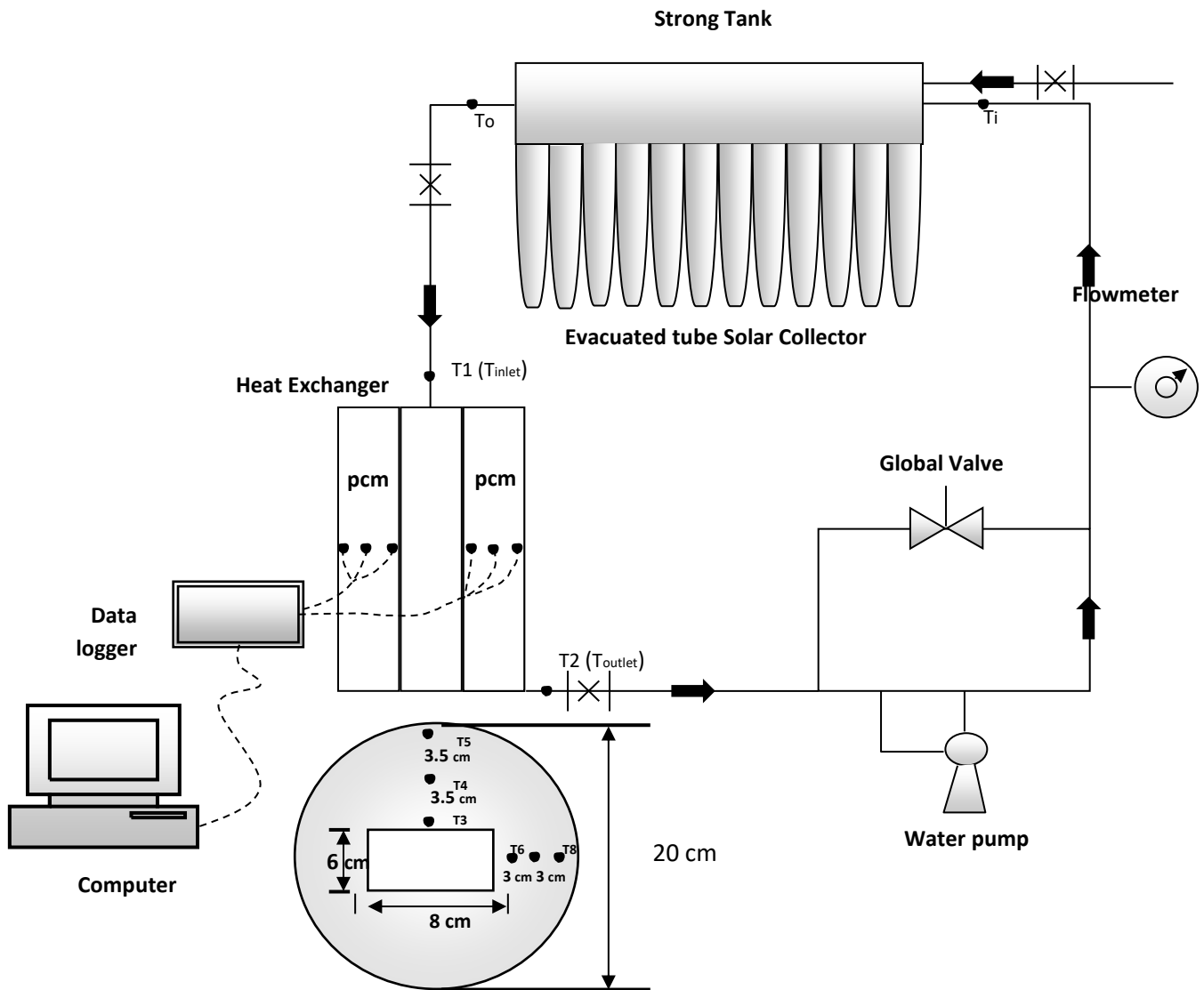


Fig. 2. A schematic diagram of the comprehensive experimental system.



Fig. 3. Melting of Paraffin (PCM) for present work.

Table 1. PCM physical properties (Abhat (1983), Lane (1983)).

| Paraffin (C₂₁ H₄₄) | Sold (12 kg) | Liquid (12 kg) |
|-------------------------------------------------|-----------------------|-----------------------|
| Density | 912 kg/m ³ | 769 kg/m ³ |
| Melting Temperature | 44.0 °C ± 0.5 | - |
| Heat Capacities | 2.4 kJ/kg·K ± 3 % | 2 kJ/kg·K ± 3 % |
| Thermal Conductivities | 0.21 W/m·K | 0.224 W/m·K |
| Heat of fusion | 189 kJ/kg | - |

2.4. Procedure of Experimental Test

The main experimental procedure in the present work is included using the solar collector type of evacuated tube for melting PCM. All experimental works were outdoor tested at AL-Mussaib city-Babylon-Iraq (Lat 32.5 ° North, and long 44.3 ° East) with N-S collector direction at tilt angle of 32.5 ° with the horizontal due to a high incident solar radiation absorbed at this angle (Ashrae, 1999). Fig. 1 shows the experimental setup of utilization the paraffins as heat energy storage in shell regime of the heat exchanger. The outer shell wall was made from aluminum as a circular cylinder shape with dimensions of 400 mm on height, 200 mm on diameter and a rectangular tube was made from stainless steel with cross section dimensions of (60 x 80) mm and 1 mm thickness wall with 400 mm height. Previously physical properties of paraffins were measured using differential scanning calorimetry (DSC) (Abhat, (1983), Lane, (1983)). 12 kg of melted paraffin was inserted in the shell regime while water flow through the tube which circulated from and to solar collector. The steps adopted for each experimental test include;

connect all thermocouples to data loggers, then adjustment date and time recorder of data loggers. Data from all thermocouples were recorded every 30 minutes then checked, fill the storage tank with source water through the intake valve, close the intake valve after the water exit from ventilation pipe, solar radiation data was recorded every 30 minute by LOGBOX data logger. The experimental tests were carried out for melting PCM, experimental data was collected from 1st of August 2017 to 31st of January 2017 as shown in [Table 2](#), each test starting at 8:00 am and terminated at 17:00 pm. Three different water circulating volume flow rates were employed through the system for every experimental stage, namely (200, 300,500) Liter per hour (LPH). The experimental tests were implemented for different weather conditions which included partly cloudy and clear sky.

Table 2. The experimental tests dates.

| Flow rate (LPH) | Summer (date) | Winter (date) |
|-----------------|----------------|---------------------|
| 200 | 5 August 2016 | 26, 27 January 2017 |
| 300 | 7 August 2016 | 28, 29 January 2017 |
| 500 | 11 August 2016 | 30, 31 January 2017 |

3. THERMAL PERFORMANCE ANALYSIS

The value of instantaneous thermal efficiency η_{th} for the water solar collector has been calculated from the energy balance of the receiver. The useful energy as heat gain (Q_u) transported to the receiver defined as ([Ma et al., 2011](#)):

$$Q_u = mc_p(T_o - T_i) \quad 1$$

Where: T_i and T_o represent the inlet fluid and exit fluid temperatures, respectively.

The instantaneous thermal efficiency of the water solar collector defined as the ratio of heat gain (Q_u) supplied to aperture area (A_a), and the solar radiation (I) which is incident on the area of aperture (A_a) ([Ma et al., 2011](#)).

$$\eta = \frac{mc_p(T_o - T_i)}{I A_a} \quad 2$$

In sensible heat storage (SHS), thermal energy is stored by raising the temperature of a solid or liquid. SHS system utilizes the heat capacity and the change in temperature of the material during the process of charging and discharging. The amount of heat stored depends on the specific heat of the medium, the temperature change and the amount of storage material, sensible heat storage system with a PCM medium is given by the following equations (Lane, 1983).

$$Q_s = mc_p(T_{in} - T_{out}) \quad 3$$

In latent heat storage system charging and discharging phenomenon occur when the storage material undergoes phase change either from solid to liquid, liquid to gaseous or solid to solid. The storage capacity of latent heat storage system with a PCM medium is given by the following equations (Lane, 1983).

$$Q = mc_{ps}(T_m - T_1) + m \cdot \Delta hm + mc_{pL}(T_f - T_m) \quad 4$$

Where T_m is melting temperature ($^{\circ}\text{C}$), C_{ps} is the average specific heat between T_1 and T_m (kJ/kg K), Δhm is heat of fusion per unit mass (J/kg) and C_{pL} is the average specific heat between T_m and T_f (J/kg K), T_1 is the initial temperature and T_f is the final temperature. In the present analysis, it considers the transport and thermal properties of the water to be dependent on the temperature as:

$$\text{Density: } \rho = 0.00001 \cdot T^3 - 0.0056 \cdot T^2 + 0.0037 \cdot T + 1000.3 \quad 5$$

$$\text{Specific heat: } C_p = -0.0000001 \cdot T^3 + 0.00003 \cdot T^2 - 0.0017 \cdot T + 4.2084 \quad 6$$

$$\text{Thermal conductivity: } k = 0.00000002 \cdot T^3 - 0.00001 \cdot T^2 + 0.0023 \cdot T + 0.5568 \quad 7$$

$$\text{Viscosity: } \mu = -0.000002 \cdot T^3 + 0.0005 \cdot T^2 - 0.0428 \cdot T + 1.6944 \quad 8$$

4. NUMERICAL SOLUTION

The geometry of the shell and tube heat exchanger is created in ANSYS-FLUENT-15. A cylindrical polar coordinate system (r, θ, z) is used with a mesh size of 8903 nodes and 12792 elements as shown in the Fig. 4. The continuity equation, momentum equation, and energy equation are (Bird et al., (1987), Bird et al., (2002)):

Continuity equation

$$\frac{\partial \rho}{\partial t} + \frac{1}{r} \frac{\partial(\rho r v_r)}{\partial r} + \frac{1}{r} \frac{\partial(\rho v_{\theta})}{\partial \theta} + \frac{\partial(\rho v_z)}{\partial z} = 0 \quad 9$$

Momentum equation

r-

$$\frac{\partial v_r}{\partial t} + v_r \frac{\partial v_r}{\partial r} + \frac{v_\theta}{r} \frac{\partial v_r}{\partial \theta} + v_z \frac{\partial v_r}{\partial z} - \frac{v_\theta^2}{r} = -\frac{1}{\rho} \frac{\partial p}{\partial r} + \frac{\mu}{\rho} \left(\frac{1}{r} \frac{\partial}{\partial r} \left(r \frac{\partial v_r}{\partial r} \right) + \frac{1}{r^2} \frac{\partial^2 v_r}{\partial \theta^2} + \frac{\partial^2 v_r}{\partial z^2} - \frac{v_r}{r^2} - \frac{2}{r^2} \frac{\partial v_\theta}{\partial \theta} \right) \tag{10}$$

$$\theta - \frac{\partial v_\theta}{\partial t} + v_r \frac{\partial v_\theta}{\partial r} + \frac{v_\theta}{r} \frac{\partial v_\theta}{\partial \theta} + v_z \frac{\partial v_\theta}{\partial z} + \frac{v_r v_\theta}{r} = -\frac{1}{\rho} \frac{\partial p}{\partial \theta} + \frac{\mu}{\rho} \left(\frac{1}{r} \frac{\partial}{\partial r} \left(r \frac{\partial v_\theta}{\partial r} \right) + \frac{1}{r^2} \frac{\partial^2 v_\theta}{\partial \theta^2} + \frac{\partial^2 v_\theta}{\partial z^2} - \frac{v_\theta}{r^2} + \frac{2}{r^2} \frac{\partial v_r}{\partial \theta} \right) \tag{11}$$

z-

$$\frac{\partial v_z}{\partial t} + v_r \frac{\partial v_z}{\partial r} + \frac{v_\theta}{r} \frac{\partial v_z}{\partial \theta} + v_z \frac{\partial v_z}{\partial z} = -\frac{1}{\rho} \frac{\partial p}{\partial z} + \frac{\mu}{\rho} \left(\frac{1}{r} \frac{\partial}{\partial r} \left(r \frac{\partial v_z}{\partial r} \right) + \frac{1}{r^2} \frac{\partial^2 v_z}{\partial \theta^2} + \frac{\partial^2 v_z}{\partial z^2} \right) \tag{12}$$

Energy equation with neglecting the viscos dissipation:

$$\rho c_p \left(\frac{\partial T}{\partial t} + v_r \frac{\partial T}{\partial r} + \frac{v_\theta}{r} \frac{\partial T}{\partial \theta} + v_z \frac{\partial T}{\partial z} \right) = k \left(\frac{\partial^2 T}{\partial r^2} + \frac{1}{r} \frac{\partial T}{\partial r} + \frac{1}{r^2} \frac{\partial^2 T}{\partial \theta^2} + \frac{\partial^2 T}{\partial z^2} \right) \tag{13}$$

Equations from (9) to (13) are solved for steady state cases by using of ANSYS-FLUENT-15. The specifications and initial and boundary conditions of the models that solved in this work are shown in Table 3.

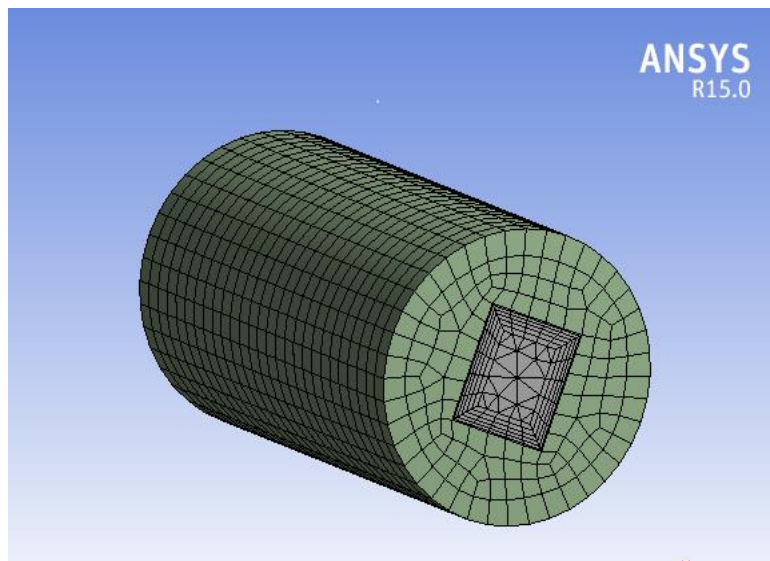


Fig. 4. Mesh generation of the present model.

Table 3. Specifications of initial and boundary conditions.

| Inner tube Specification | Inlet Temperature, °C | Flow Regime; Inner tube | Turbulence intensity, % |
|--------------------------|-----------------------|-------------------------|-------------------------|
| Value | 55 | Turbulent; Re=15000 | 5 |

5. RESULTS

5.1. Collector performance

Fig. 5 displays the experimental results of the solar radiation power per square meter that falls on the present solar collector for selected clear days on August 2016 at test position. It can be exposed that the solar radiation is increased from low values at morning to maximum values on the noon then decrease to low values on the afternoon. The comparison of the solar radiation measured data for two clear days shows the same behavior due to no cloud and dust in the sky. Fig. 6 illustrates the day hourly variation of the solar collector thermal efficiency on August 2016 for two tests days. It indicated the thermal efficiency increased till 12:30 pm after that it is decreased.

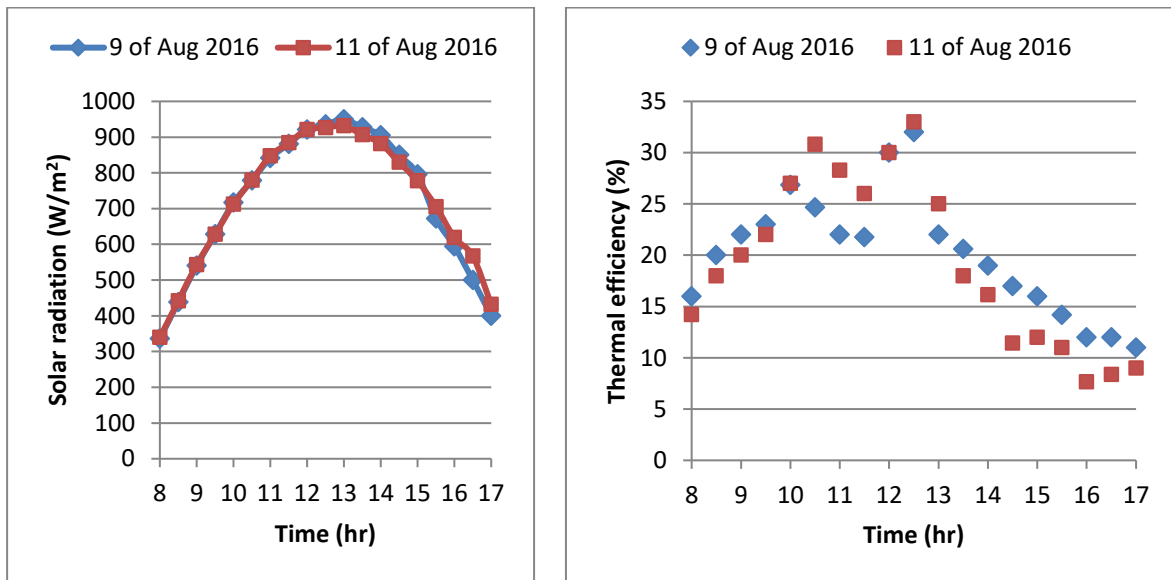


Fig. 5. Solar radiation on 9 and 11 Aug. 2016. Fig. 6. Collector efficiency on 9 and 11 Aug. 2016.

The operation curve for the tests on two clear days is exposed in Figs. 7 and 8. The thermal efficiency of the ETSC system is found by computing the instantaneous thermal efficiency for high values of incident solar radiation, water temperature in the collector, ambient temperatures. This wanted experimentally measured of the incident solar radiation onto ETSC under quasi-steady state conditions. That's occurs over the period from 11:00 am to 14:00 pm. The relationship between the thermal efficiency and $(T_i - T_a)/I$ found as:

For 9 Aug. 2016

$$\eta_{th} = 0.3432 - 15.716\left(\frac{T_i - T_a}{I}\right)$$

For 11 Aug. 2016

$$\eta_{th} = 0.3309 - 4.8801\left(\frac{T_i - T_a}{I}\right)$$

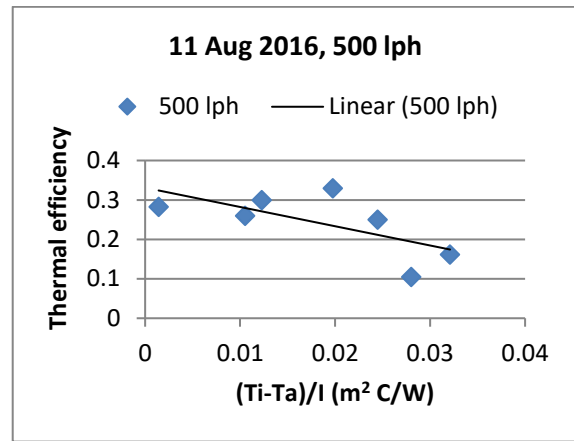
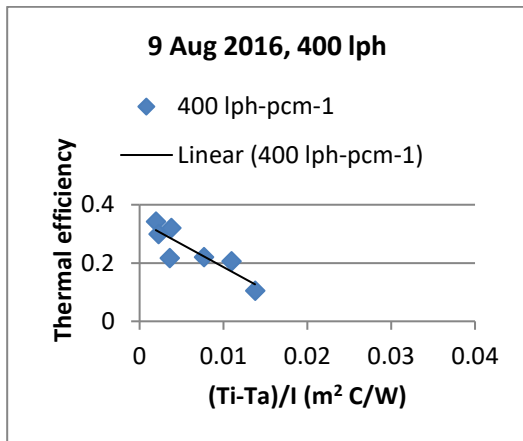


Fig. 7. Operation curve of Solar Collector for 400 lph. Fig. 8. Operation curve of Solar Collector for 500 lph.

5.2. PCM

All experimental tests for PCM are done on the same summer season; on the August month 2016, then all the experimental tests for that done on the summer reason are redone on the winter season; on January 2017. Figs. 9 and 10 shows the relation between water inlet temperatures of inner tube (T_{in}) and the PCM temperatures ($T_3, T_4, T_5, T_6, T_7,$ and T_8) versus hourly time for a water flow rates of 200 lph and 300 lph on 5th and 7th August 2016 respectively in the different angular direction. The water inlet temperature is noticed to be higher than the highest temperature of PCM. It can be shown that the inlet water temperature and all the PCM temperatures are increased from 8:00 am to 17:00 pm due to increasing in the thermal energy observed from the solar radiation. The maximum temperatures of inlet water to inner tube and PCM are 73 °C and 64 °C for water flow rate of 200 lph respectively occurs at 17:00 pm, also 67.8 and 54.2 for water flow rate of 300 lph at the same time due to the radiation energy absorbed by solar collector for 200 lph is higher than for 300 lph because of high radiation on the day test for 200 lph. It can be shown the melting process occurs at 12:00 noon for water flow rate of 200 lph and at 13:00 pm for water flow rate of 300 lph due to the storage heat of 200 lph is higher than 300 lph, that mean the melting point needed only 3-4 hours to reach. Figs. 11 and 12 shows more details of the relation between water inlet temperature of inner tube and the PCM temperatures versus hourly time for a water flow rate of 200 lph on Aug 2016. One may observe that T_3 and T_6 are highest temperatures for PCM because of it are closest to inner tube surface that lead to increase the heat transfer at this locations faster than at the locations of $T_4, T_5, T_7,$ and T_8 . Also, it can be shown that T_3 is higher than T_6 because

of the contact area of the PCM near T3 is more than T6 and unsymmetrical in its locations from the bulk temperature of water flow inside rectangular inner tube.

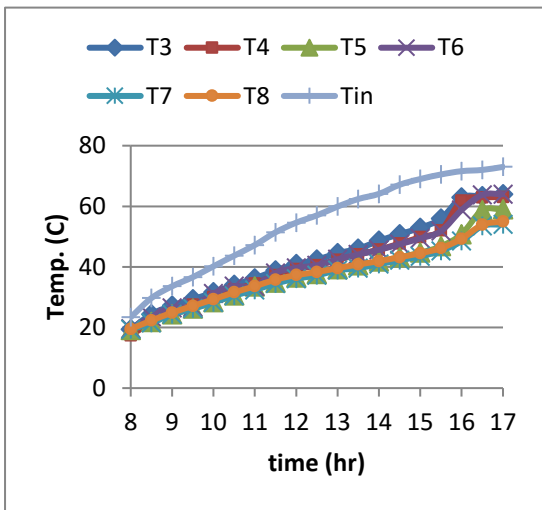


Fig. 9. PCM temperatures (200 lph-5Aug 2016).

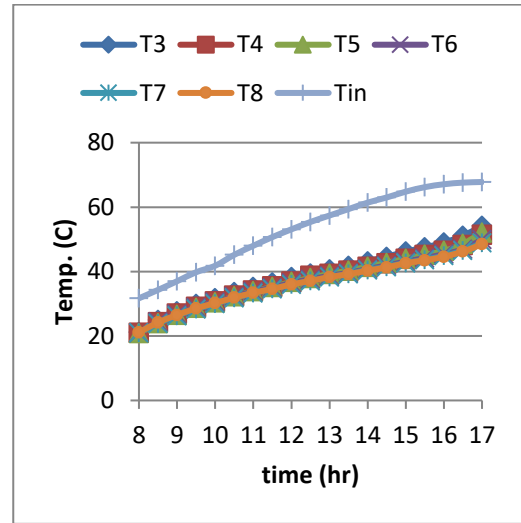


Fig. 10. PCM temperatures (300 lph-7Aug 2016).

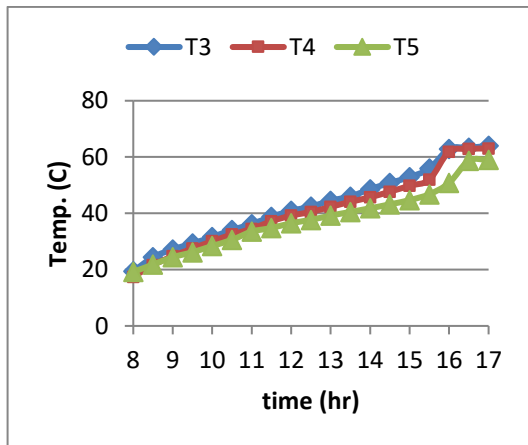


Fig. 11. (T3, T4, T5) (200 lph-5Aug 2016).

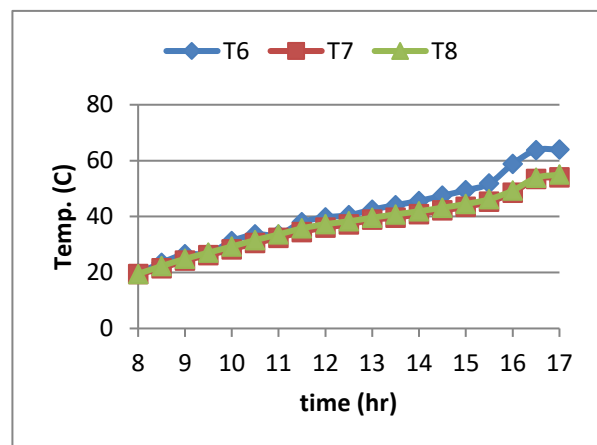


Fig. 12. (T6, T7, T8) (200 lph-5Aug 2016).

Fig. 13 shows the relation between middle temperature (T4) of PCM versus hourly time for a water flow rates of 200, 300, and 500 lph on Aug 2016. It can be observed that the temperatures for the flow rate of 500 lph are highest temperatures than temperatures of the lower flow rates (200, 300) lph, because of the solar energy and inlet temperatures for 500 lph water flow rate inside inner tube have highest values than solar energy and inlet temperatures of the lower flow rates (200, 300) lph as shown in Fig. 14. Fig. 14 shows the relation between the Inlet water temperature inside inner tube (Tin) versus hourly time for a water flow rates of 200, 300, and 500 lph on Aug 2016. It can be detected that the temperatures for the flow rate of 500 lph are highest temperatures than temperatures of the lower flow rates (200, 300) lph, due to the ambient temperatures for 500 lph water flow rate inside inner tube have highest temperatures than ambient temperatures of the lower flow rates (200, 300) lph as shown in Fig. 15. Fig. 15

shows the ambient temperature with daily time for three days on August 2016, which represented a test days for 200, 300, and 500 lph.

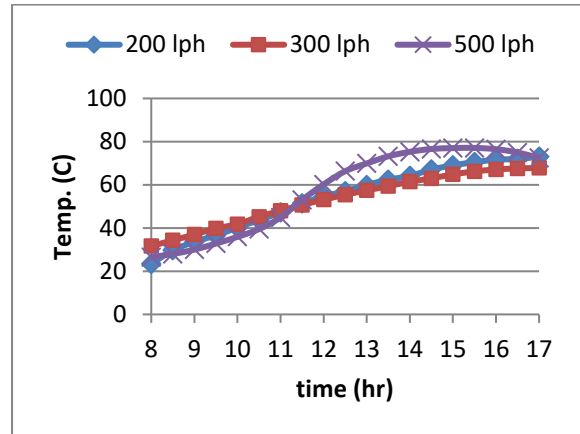
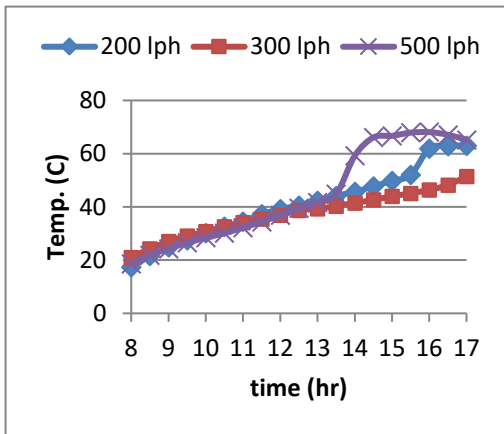


Fig. 13. PCM middle temperatures (T_4) on Aug 2016. Fig. 14. Inlet water temperature (T_{in}) on Aug 2016

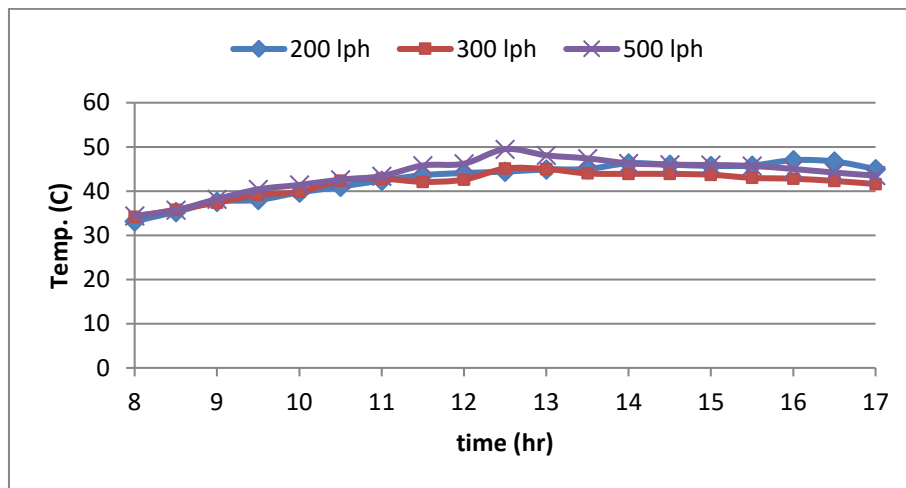


Fig. 15. Ambient temperature (T_{amb}) on Aug 2016.

Fig. 16 shows the relation between the heat energy gained from the hot water flow inside inner tube versus hourly time for a water flow rates of 200, 300, and 500 lph on Aug 2016. It can be observed that the heat gained for the flow rate of 200 lph are highest temperatures than that of the others flow rates (300, 500) lph, due to the solar energy and temperatures differences for 200 lph water flow rate inside inner tube have highest values than that of the others flow rates (300, 500) lph as shown in Fig. 17.

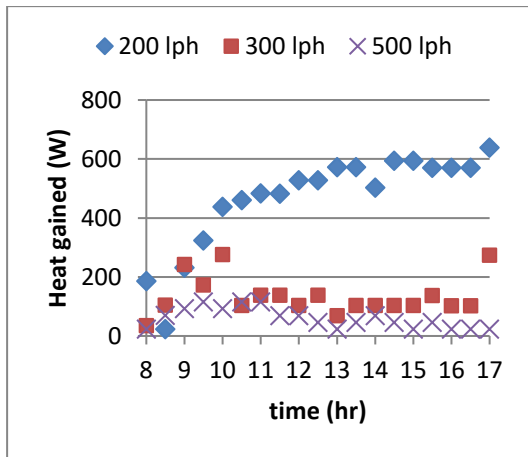


Fig. 16. Heat gained for PCM on Aug 2016.

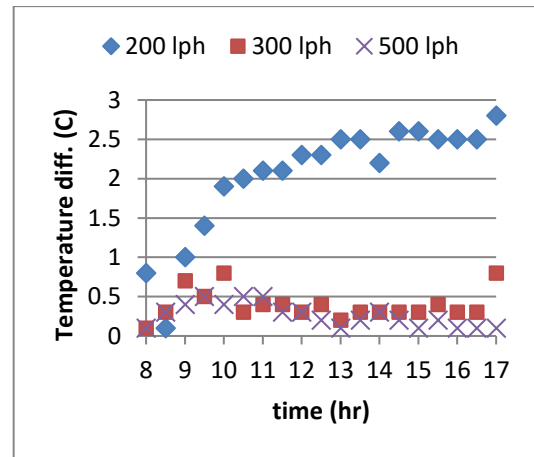


Fig. 17. Water temp. Difference of inner tube for PCM on Aug. 2016.

Fig. 18 shows the relation between the raise of temperature for middle sensor (T4) for PCM versus hourly time for a water flow rates of 200, 300, and 500 lph on Aug. 2016. It can be observed that the maximum raising temperature is 14.2 °C found for the flow rate of 500 lph at 14:00 pm. These values are measured every half hour along daily test time. Fig. 19 shows the relation between the raise percent of temperature for middle sensor (T4) for PCM1 versus hourly time for a water flow rates of 200, 300, and 500 lph on Aug. 2016. It can be observed that the maximum raising percent of temperature is 32% found for the flow rate of 500 lph at 14:00 pm. The percent values are measured every half hour along daily test time.

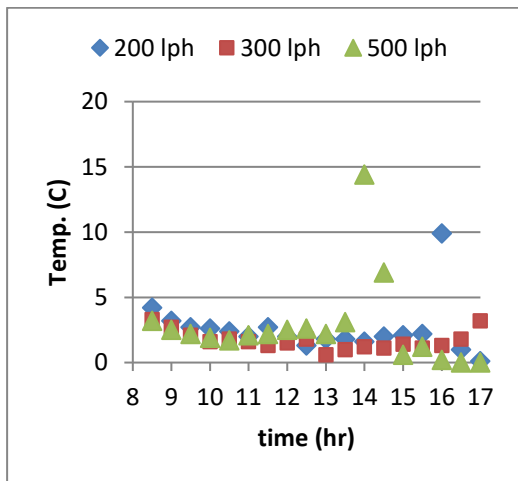


Fig. 18. Raising of (T4) for PCM on Aug. 2016.

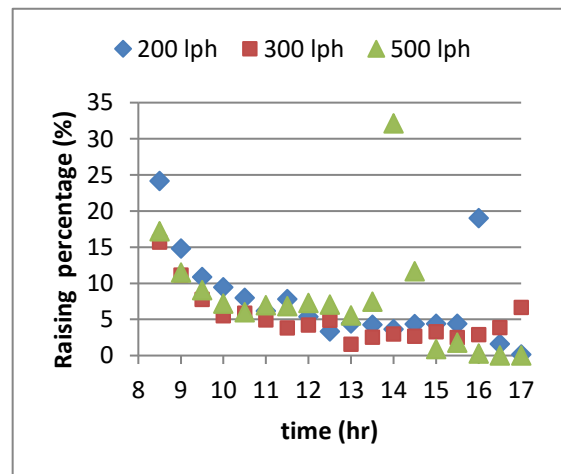


Fig. 19. Raising percentage of (T4) for PCM on Aug. 2016.

Fig. 20 shows the relation between the middle temperatures (T4) of PCM versus hourly time for a water flow rates of 200, 300, and 500 lph on (winter season) Jan. 2017. In winter season every flow rate take place along two days to reach a melting temperature of PCM. It can be observed that the temperatures for the flow rate of 500 lph are highest temperatures than temperatures of the lower flow rates (200, 300) lph, because of the inlet temperatures for 500

lph water flow rate inside inner tube have highest temperatures than inlet temperatures of the lower flow rates (200, 300) lph as shown in Fig. 21. Fig. 21 shows the relation between the Inlet water temperature inside inner tube (T_{in}) for PCM versus hourly time for a water flow rates of 200, 300, and 500 lph on Jan. 2017. It can be detected that the temperatures for the flow rate of 500 lph are highest temperatures than temperatures of the lower flow rates (200, 300) lph, due to the ambient temperatures for 500 lph water flow rate inside inner tube have highest temperatures than ambient temperatures of the lower flow rates (200, 300) lph.

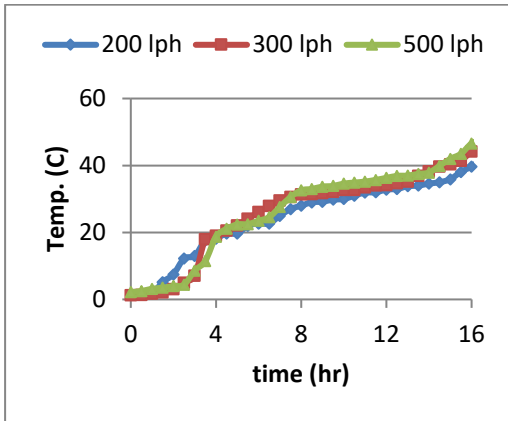


Fig. 20. PCM (T_4) on Jan. 2017.

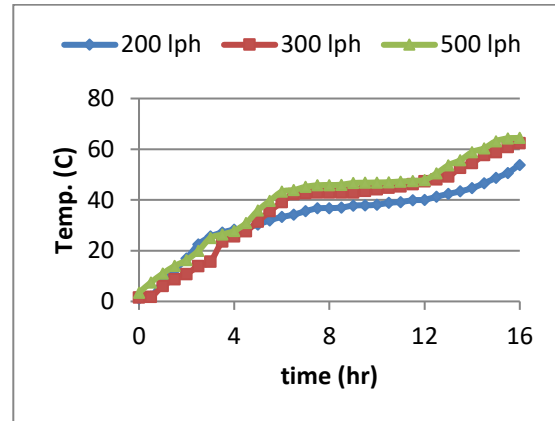


Fig. 21. Inlet water temperature (T_{in}) for PCM on Jan. 2017.

Fig. 22 shows the relation between the heat energy gained from the hot water flow inside inner tube for PCM1 versus hourly time for a water flow rates of 200, 300, and 500 lph on Jan. 2017. It can be observed that the heat gained for the flow rate of 500 lph are highest temperatures than that of the others flow rates (200, 300) lph, due to the temperatures differences for 500 lph water flow rate inside inner tube have highest values than that of the others flow rates (200, 300) lph as shown in Fig. 23.

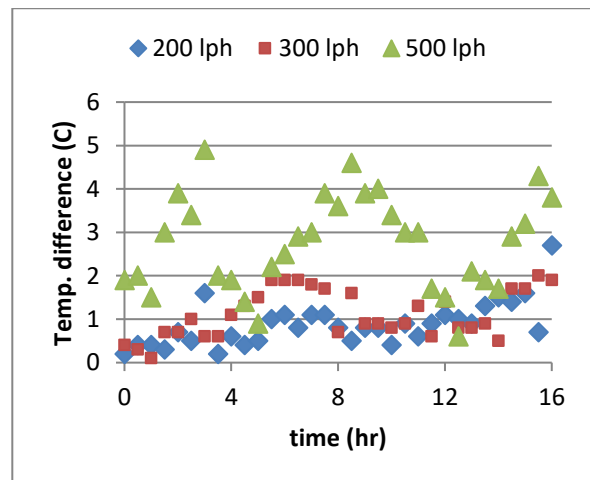
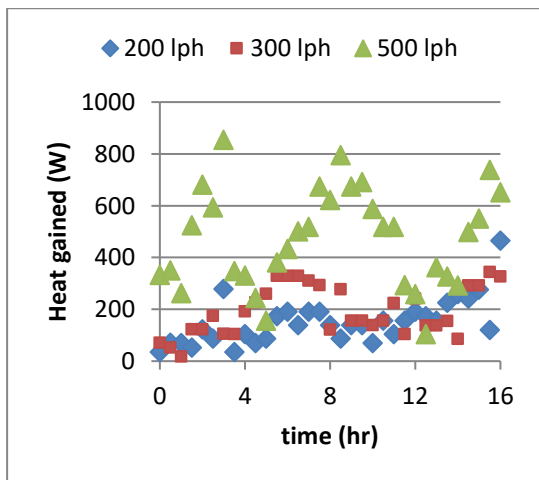


Fig. 22. Heat gained for PCM on Jan. 2017. Fig. 23. Water temp. Difference of inner tube for PCM on Jan. 2017.

Fig. 24 shows the relation between the raise of temperature for middle sensor (T4) for PCM versus hourly time for a water flow rates of 200, 300, and 500 lph on Jan. 2017. It can be observed that the maximum raising temperature is 4.7 °C found for the flow rate of 200 lph. These values are measured every half hour along daily test time. Fig. 25 shows the relation between the raise percent of temperature for middle sensor (T4) for PCM1 versus hourly time for a water flow rates of 200, 300, and 500 lph on Jan. 2017. It can be observed that the maximum raising percent of temperature is 63% found for the flow rate of 200 lph. The percent values are measured every half hour along daily test time.

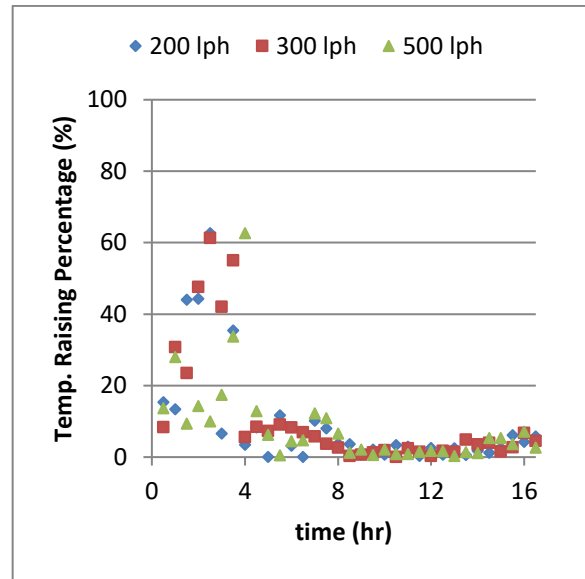
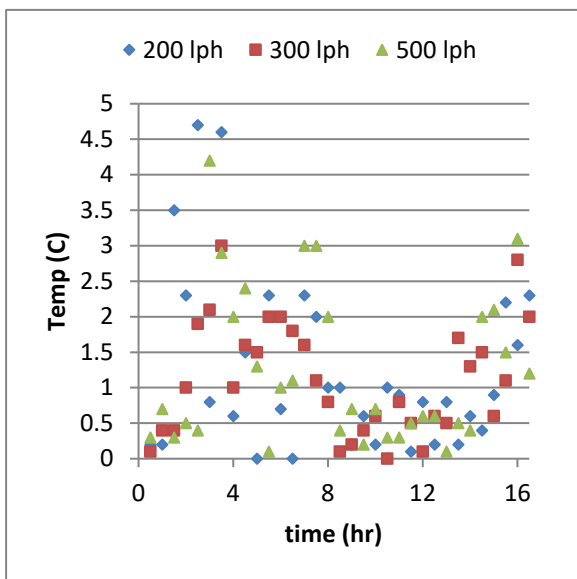


Fig. 24. Raising (T4) for PCM on Jan. 2017.

Fig. 25. Raising percentage of (T4) for PCM on Jan. 2017.

Fig. 26 shows the relationship between the latent heat of (PCM) versus discharge rates of water flow from 200, 300, and 500 lph on summer season and winter season. Each point represented a latent heat of completely flow rate test. It can results indicate that the heat stored in the flow rate 300 lph on winter is the highest heat stored of other flow (200, 500), due to 200 lph have a maxim temperature difference between initial temperature and final temperature, which have initial temperature 1.2°C and the final temperature (46.2°C).

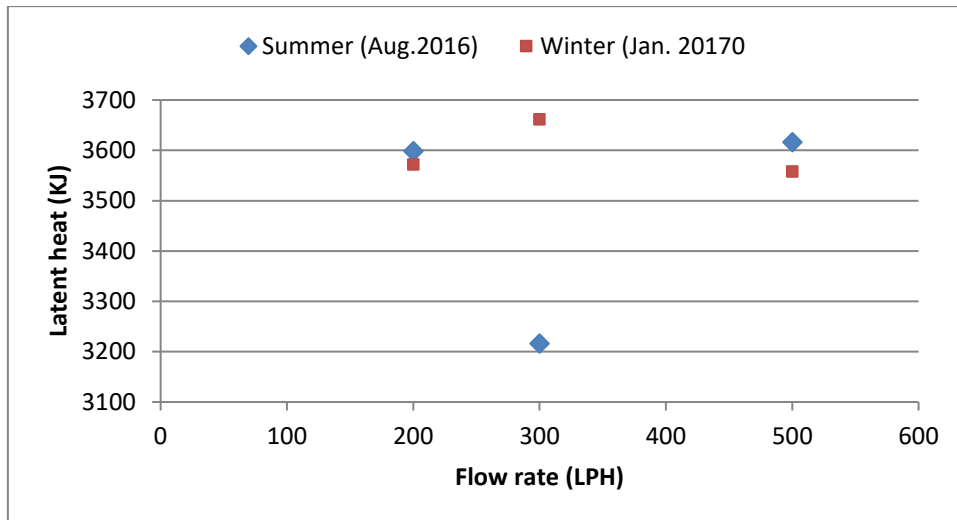


Fig. 26. Latent heat of PCM.

5.3. Numerical Results

The numerical results are obtained by employing ANSYS Fluent 15.0 software that demonstrated in section (4) for examine the effect of geometry and conditions of flow on thermal characteristics of PCM, the geometries and condition of the model for the present work are given in Table 2. One model of shell and tube is tested numerically for steady state, turbulent flow.

Static temperature contour of the PCM for the Reynolds Number of 15000 is given in Fig. 27, the effect of cross heat transfer in the shell region is visible from the temperature contour. It can be shown that the temperature at inner tube is higher than PCM temperature in the shell side and there is no symmetric distribution of PCM temperature due to rectangular shape of inner tube.

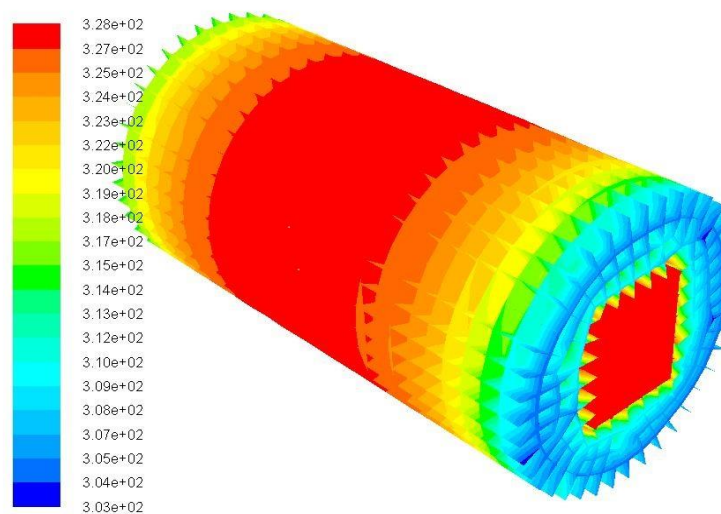


Fig. 27. Static temperature contour.

The results of the analysis of the numerical simulation are used to estimate the PCM temperature distribution. Fig. 28 gives a comparison of the temperature distributions obtained from the experiment and those obtained by using the numerical simulation in the different angular directions. The same inlet boundary conditions are employed for numerical model and experimental tests. The comparison gave good validation with small mean difference; the percentage deviation for temperatures is 2% for (T3, T4, and T5) direction and 2.7% for (T6, T7, and T8) direction. The comparison shows a good agreement between the computational and experimental values which indicated that the present numerical models can be used to compute the performance of system.

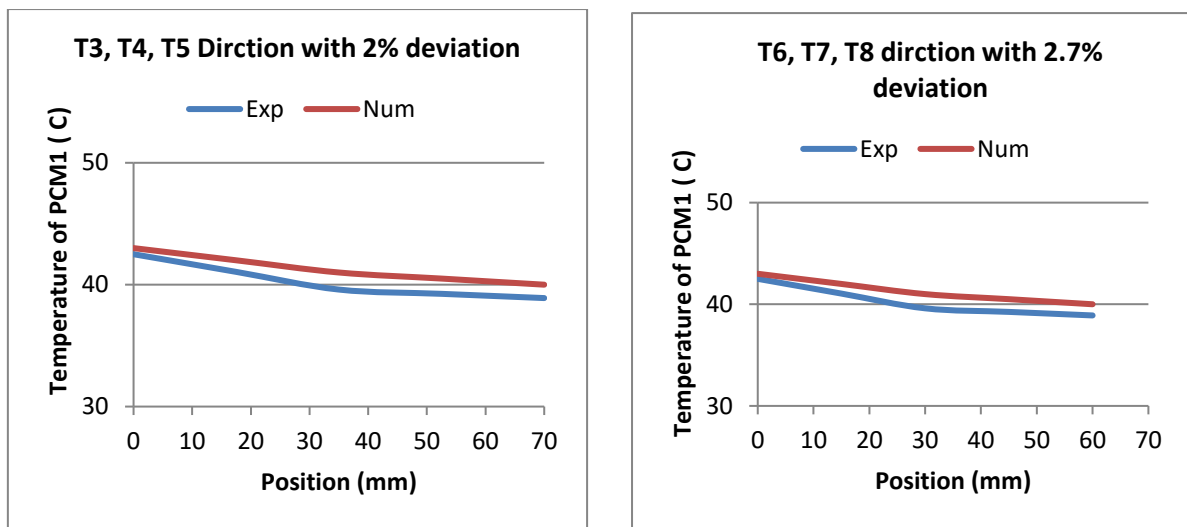


Fig. 28. Experimental and numerical comparison of PCM temperature distribution.

Verifying of the results obtained of the present work is compared with that achieved by previous studies. Fig. 29 shows a comparison of PCM middle temperature of the present work with inner flow rate of 200 lph with results reported by [yongcai Li, \(2013\)](#) for melting under a group of light radiation in the laboratory. The comparison is given a good agreement with increasing for present work of 25.9 %.

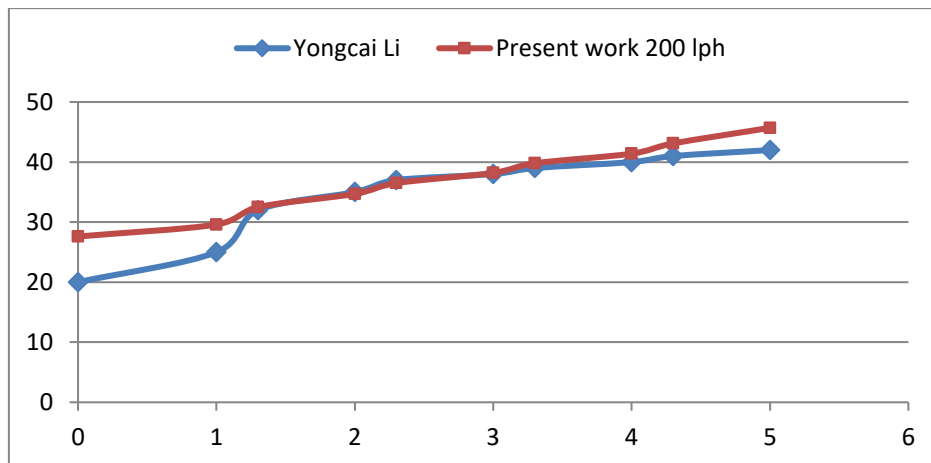


Fig. 29. Compares on between the present work and [yongcai Li (2013)].

6. CONCLUSIONS

The melting processes in a shell and tube heat exchanger by using solar thermal energy have been investigated numerically and experimentally. The PCM that employed in this work is black color Iraqi origin pure Paraffin (PCM) with amount of 12 kg. The main experimental procedure in the present work is included using the solar collector type of evacuated tube for melting PCM in shell regime. Different volume flow rates for the water inside the inner tube of heat exchanger for Reynolds number namely (15000, 23000, 38000) were studied. The influence of the inner tube inlet and ambient temperatures were investigated. The results indicated that the inner tube inlet and ambient temperatures has a significant effects on the melting process compared with the volume flow rates. Studying PCM temperature distribution, it is exposed that a melting temperature of the PCM in summer season needed time of (3-4) hours only, while it needed more time (14-16) hours in winter season. Increasing solar radiation and ambient temperature reduces the melting time for both PCM types. Increasing water temperature difference of inner tube increased the heat gained for PCM.

7. REFERENCES

- Abhat A. Low temperature latent heat thermal energy storage: heat storage materials. *Sol Energy*. 30:313–32, 1983.
- ASHRAE applications Handbook, Chapter 32 by American Society of Heating, Solar energy Use. Atlanta, GA: 1999.
- Atul Sharma, C. R. Chen, Solar Water Heating System with Phase Change Materials, *International Review of Chemical Engineering (I.RE.CH.E.)*, Vol. 1, N. 4 July 2009.

Vasishta D. Bhatt, Kuldip Gohil, Arunabh Mishra "Thermal Energy Storage Capacity of some Phase changing Materials and Ionic Liquids" *International Journal of ChemTech Research* CODEN(USA): ISSN : 0974-4290 Vol.2, No.3, pp 1771-1779, July-Sept 2010.

D. Fernandez Thermal energy storage: "How previous findings determine current research priorities" *Energy* 39, 246 -275, 2012.

J. Ma, W. Sun, J. Ji, Y. Zhang, A. Zhang, and W Fan. "Experimental and theoretical study of the efficiency of a dual function solar collector". *Applied Thermal Engineering*, 31: 1751–1756, 2011.

Lane GA. *Solar Heat Storage Latent heat materials*, vol.1. Boca Raton FL: CRC Press, Inc.; 1983

M.Ravikumar and DR.Pss, *Phase change material as a thermal energy for cooling of Joint*. All rights reserved, 2008.

Murat Kenisarin, Khamid Mahkamov, *Solar energy storage using phase change materials*, 11, 1913–1965, 2007.

R. B. Bird, R. C. Armstrong, and O. Hassager, *Dynamics of Polymeric Fluids: Volume 1 Fluid Mechanics*, Wiley: NY, 1987.

R. B. Bird, W. E. Stewart, and E. N. Lightfoot, *Transport Phenomena*, 2nd edition, Wiley: NY, 2002.

Ronald Warzoha, Omar Sanusi, Brian McManus, Amy S. Fleischer, *Evaluation of Methods to Fully Saturate Carbon Foam with Paraffin Wax Phase Change Material for Energy Storage*, 978-1-4244-9532-0/12, 2012.

Sekar Sinaringati, Nandy Putra, Muhammad Amin and Fitri Afriyanti, *The Utilization of paraffin and beeswax as heat energy storage in infant incubator*, vol.11.NO.2, January 2016.

Shuo Peng,¹ Alan Fuchs,¹ R. A. Wirtz² *Polymeric Phase Change Composites for Thermal Energy Storage* , 19 January 2004.

Yongcai Li, thesis, *Thermal Performance Analysis of A PCM Combined Solar Chimney System for Natural Ventilation and Heating/Cooling* , September, 2013.